

available at [www.sciencedirect.com](http://www.sciencedirect.com)journal homepage: [www.ejconline.com](http://www.ejconline.com)

## **<sup>89</sup>Zr-trastuzumab PET visualises HER2 downregulation by the HSP90 inhibitor NVP-AUY922 in a human tumour xenograft**

Thijs H. Oude Munnink <sup>a,g</sup>, Maarten A. de Korte <sup>a,g</sup>, Wouter B. Nagengast <sup>a</sup>,  
Hetty Timmer-Bosscha <sup>a</sup>, Carolina P. Schröder <sup>a</sup>, Johan R. de Jong <sup>b</sup>,  
Guus A.M.S. van Dongen <sup>c</sup>, Michael Rugaard Jensen <sup>d</sup>, Cornelia Quadt <sup>e</sup>,  
Marjolijn N. Lub-de Hooge <sup>b,f</sup>, Elisabeth G.E. de Vries <sup>a,\*</sup>

<sup>a</sup> Department of Medical Oncology, University of Groningen and University Medical Centre Groningen, Hanzeplein 1, 9713 GZ Groningen, The Netherlands

<sup>b</sup> Department of Nuclear Medicine and Molecular Imaging, University of Groningen and University Medical Centre Groningen, Hanzeplein 1, 9713 GZ Groningen, The Netherlands

<sup>c</sup> Department of Nuclear Medicine and PET Research, VU University Medical Centre, De Boelelaan 1117, 1081 HV Amsterdam, The Netherlands

<sup>d</sup> Novartis Institute for Biomedical Research, Klybeckstrasse 141, CH-4057 Basel, Switzerland

<sup>e</sup> Novartis Pharma, Lichtstrasse 35, CH-4002 Basel, Switzerland

<sup>f</sup> Department of Hospital and Clinical Pharmacy, University of Groningen and University Medical Centre Groningen, Hanzeplein 1, 9713 GZ Groningen, The Netherlands

### ARTICLE INFO

#### Article history:

Received 23 September 2009

Received in revised form 18

November 2009

Accepted 1 December 2009

Available online 24 December 2009

#### Keywords:

HER2

Heat shock protein 90

NVP-AUY922

Zirconium-89

Positron emission tomography

Breast cancer

Biomarker

### ABSTRACT

NVP-AUY922, a potent heat shock protein (HSP) 90 inhibitor, downregulates the expression of many oncogenic proteins, including the human epidermal growth factor receptor-2 (HER2). Because HER2 downregulation is a potential biomarker for early response to HSP90-targeted therapies, we used the <sup>89</sup>Zr-labelled HER2 antibody trastuzumab to quantify the alterations in HER2 expression after NVP-AUY922 treatment with HER2 positron emission tomography (PET) imaging.

The HER2 overexpressing human SKOV-3 ovarian tumour cell line was used for *in vitro* experiments and as xenograft model in nude athymic mice. *In vitro* HER2 membrane expression was assessed by flow cytometry and a radio-immuno assay with <sup>89</sup>Zr-trastuzumab. For *in vivo* evaluation, mice received 50 mg/kg NVP-AUY922 intraperitoneally every other day. <sup>89</sup>Zr-trastuzumab was injected intravenously 6 d before NVP-AUY922 treatment and after 3 NVP-AUY922 doses. MicroPET imaging was performed at 24, 72 and 144 h post tracer injection followed by ex-vivo biodistribution and immunohistochemical staining.

After 24 h NVP-AUY922 treatment HER2 membrane expression showed profound reduction with flow cytometry (80%) and radio-immuno assay (75%). PET tumour quantification, showed a mean reduction of 41% (*p* = 0.0001) in <sup>89</sup>Zr-trastuzumab uptake at 144 h post tracer injection after NVP-AUY922 treatment. PET results were confirmed by ex-vivo <sup>89</sup>Zr-trastuzumab biodistribution and HER2 immunohistochemical staining.

\* Corresponding author. Address: Department of Medical Oncology, University Medical Centre Groningen, P.O. Box 30.001, 9700 RB Groningen, The Netherlands. Tel.: +31 50 361 2821; fax: +31 50 361 4862.

E-mail address: [e.g.e.de.vries@int.umcg.nl](mailto:e.g.e.de.vries@int.umcg.nl) (E.G.E. de Vries).

<sup>g</sup> Contributed equally.

0959-8049/\$ - see front matter © 2009 Elsevier Ltd. All rights reserved.

doi:10.1016/j.ejca.2009.12.009

NVP-AUY922 effectively downregulates HER2, which can be monitored and quantified *in vivo* non-invasively with  $^{89}\text{Zr}$ -trastuzumab PET. This technique is currently under clinical evaluation and might serve as an early biomarker for HSP90 inhibition in HER2 positive metastatic breast cancer patients.

© 2009 Elsevier Ltd. All rights reserved.

## 1. Introduction

Heat shock protein 90 (HSP90) is a 90 kDa molecular chaperone protein which is involved in the conformation, activation, functionality and stability of over 100 client proteins. Client proteins of HSP90 are involved in all hallmarks of oncogenesis: tumour cell growth, invasion, metastasis, angiogenesis, evading apoptosis and insensitivity to anti-growth signals.<sup>1</sup> Tumour cells overexpress HSP90 2- to 10-fold compared to normal cells of the related tissue and are more dependent on HSP90 than normal counterparts.<sup>2</sup> In tumour cells HSP90 is predominantly present in an active complexed state with a higher ATPase activity and ATP affinity.<sup>3</sup> These characteristics make HSP90 a target with high potential for cancer therapy, as the inhibition of HSP90 results in targeting multiple signalling pathways crucial for tumour maintenance.

Several HSP90 inhibitors are currently in clinical development. Most pre-clinical and clinical experience has been obtained with the geldanamycin class of HSP90 inhibitors of which 17-(allylamino)-17-demethoxygeldanamycin (17-AAG; tanespimycin) is the best-studied family member. Therapeutic effects (disease stabilization, tumour responses) of 17-AAG were seen in several phase I and II trials, including a phase II trial in patients refractory to trastuzumab therapy.<sup>4,5</sup> However, clinical application of 17-AAG is hampered due to hepatotoxicity and formulation difficulties.

A new interesting class of HSP90 inhibitors consists of the pyrazole resorcinols, of which NVP-AUY922 is *in vitro* the most potent family member.<sup>6</sup> Pre-clinical activity of NVP-AUY922 has been reported recently<sup>7,8</sup> and NVP-AUY922 is currently being investigated in two phase I-II clinical trials.

Monitoring the pharmacodynamic effects of HSP90 inhibitors would facilitate the clinical development of these drugs. Currently there is no proven early biomarker for evaluating HSP90 inhibition. In a clinical phase I study with 17-AAG, tumour biopsies were taken in which Western blot analysis revealed c-RAF1 inhibition, CDK4 depletion and HSP70 induction.<sup>4</sup> The limited feasibility of repeated tumour biopsies, however, has driven the search for non-invasive pharmacodynamic monitoring of HSP90 inhibitors.<sup>9</sup>

One of the most potent oncogenic client proteins of HSP90 is the human epidermal growth factor receptor-2 (HER2). HER2 is a key player in oncogenic transformation in a variety of cancer types and is overexpressed in 20–25% of breast cancers.<sup>10</sup> The rapid but transient HER2 degradation induced by HSP90 inhibition has been shown *in vitro* and *in vivo* in several pre-clinical reports.<sup>7,8,11,12</sup>

Molecular imaging techniques are well suited for non-invasive monitoring of the rapid molecular changes induced by tumour-targeting therapies. Serial HER2 positron emission

tomography (PET) imaging is potentially attractive as biomarker as it allows the visualisation and quantification of the molecular tumour response to the drug early during treatment.

HER2 PET imaging with a  $^{68}\text{Ga}$ -labelled trastuzumab  $F(ab')_2$  fragment ( $^{68}\text{Ga}$ -DCHF) has preclinically shown to be able to monitor the HER2 downregulation after 17-AAG treatment.<sup>13</sup> In the search for a clinical usable PET tracer, we labelled the HER2 full length antibody trastuzumab with the long-lived PET isotope zirconium-89 ( $^{89}\text{Zr}$ ) for HER2 PET imaging. The pre-clinical kinetics and biodistribution of  $^{89}\text{Zr}$ -trastuzumab have recently been described.<sup>14</sup> Our clinical experience with this tracer for HER2 imaging in metastatic breast cancer patients showed excellent feasibility.<sup>15</sup> In the present study, we aim to use  $^{89}\text{Zr}$ -trastuzumab PET imaging for non-invasive quantification of the HER2 downregulation by the HSP90 inhibitor NVP-AUY922 in a HER2 positive xenograft model.

## 2. Materials and methods

### 2.1. Cell line and reagents

The HER2 overexpressing human ovarian cancer cell-line SKOV-3 was obtained from American Type Culture Collection. Cells were cultured in a humidified incubator at 5%  $\text{CO}_2$  and 37 °C in D-MEM high glucose, supplemented with 10% FCS. NVP-AUY922 was provided by Novartis. 17-AAG was purchased from LC Laboratories and was used as a reference for the *in vitro* effects of NVP-AUY922. For the *in vitro* experiments NVP-AUY922 and 17-AAG were dissolved in DMSO and stored at –80 °C or –20 °C, respectively. For intraperitoneal (i.p.) administration, NVP-AUY922 was dissolved in 5% glucose and was delivered in a volume of 200  $\mu\text{L}$ . *In vivo* experiments were performed with NVP-AUY922 only.

### 2.2. Flow cytometry

Attached cells were incubated with 30 or 100 nM NVP-AUY922 for 24 h. In these concentrations, NVP-AUY922 was shown to downregulate HER2 expression *in vitro*.<sup>7,8</sup> For reference, cells were also incubated with 30, 100 or 500 nM 17-AAG. Cells were harvested with trypsin, washed and diluted in cold phosphate buffered saline (PBS). Subsequently, cells were incubated on ice for 45 min with 20  $\mu\text{g}/\text{mL}$  trastuzumab followed by 45 min with 20  $\mu\text{g}/\text{mL}$  monoclonal anti-human IgG, FITC conjugated (Clone HP 6017, Sigma). Membrane receptor expression was analysed using flow cytometry (FACSCalibur, BD Biosciences) with Winlist software (Verity Software House). For every treatment condition, three independent experiments were performed.

### 2.3. Conjugation and $^{89}\text{Zr}$ -labelling of trastuzumab

Trastuzumab (Herceptin, Roche) conjugation and labelling was performed as described previously.<sup>14</sup> Briefly, trastuzumab was first conjugated with the chelator N-succinyl-desferrioxamine B-tetrafluorophenol (N-sucDf-TFP) (VUMC). After conjugation, the product was purified by ultracentrifugation and stored at  $-20^\circ\text{C}$ . In the second step, N-sucDf-trastuzumab was radiolabelled with clinical-grade  $^{89}\text{Zr}$  oxalate (IBA Molecular).

### 2.4. Conjugation and $^{111}\text{In}$ -labelling of control human IgG

Human IgG (Sanquin) conjugation and labelling was performed according to Ruegg.<sup>14,16</sup> Briefly, IgG was first conjugated to the bifunctional conjugating agent 2-(4-isothiocyanatobenzyl)-diethylenetriaminepentaacetic acid (p-SCN-Bn-DTPA, Macrocyclics). After conjugation, the product was used for radiolabelling immediately or stored at  $-20^\circ\text{C}$ . Conjugated human IgG was radiolabelled with  $^{111}\text{InCl}_3$  (Covidien). Glassware, materials and solutions used for the conjugation and labelling procedures were sterilized, pyrogen-free and metal-free.

### 2.5. Radio-immuno assay

Attached cells were incubated with 30 or 100 nM NVP-AUY922 or 500 nM 17-AAG for 24 h. Cells were harvested following trypsinisation and were washed and diluted in cold PBS. To correct for aspecific binding, a sample of the untreated cells was blocked with a 500-fold excess of unlabelled trastuzumab. For each condition,  $5 \times 10^5$  cells were incubated in triplicate for 60 min with  $1 \mu\text{g}$   $^{89}\text{Zr}$ -trastuzumab at  $4^\circ\text{C}$ . Binding of  $^{89}\text{Zr}$ -trastuzumab was measured in a calibrated well-type LKB-1282-Compu-gamma system (LKB Wallac). For every treatment condition, three independent experiments were performed.

### 2.6. Animal studies

*In vivo* imaging and biodistribution experiments were conducted using male athymic mice (Hsd:Athymic Nude/nu) obtained from Harlan. Mice were injected subcutaneously with  $10^6$  SKOV-3 cells mixed equally with Matrigel™ (BD Bioscience). When tumours measured between 5 and 8 mm in diameter ( $\sim 0.2 \text{ cm}^3$ ), approximately 2–3 weeks after inoculation, mice were injected with a  $^{89}\text{Zr}$ -trastuzumab ( $100 \mu\text{g}, \pm 5 \text{ MBq}$ ) and IgG ( $100 \mu\text{g}$ ) co-injection via the penile vein. Animals were imaged using a MicroPET Focus 220 rodent scanner (CTI Siemens). Static images of 15–45 min acquisition time were obtained at 24, 72 and 144 h post injection. NVP-AUY922 was administered i.p. every other day in a dose of 50 mg/kg starting directly after the 144 h scan of the baseline  $^{89}\text{Zr}$ -trastuzumab injection. With this treatment regimen, NVP-AUY922 has shown to decrease HER2 tumour expression and to effectively inhibit tumour growth *in vivo*, with acceptable tolerability.<sup>8</sup> After three doses of NVP-AUY922, mice were again injected with  $^{89}\text{Zr}$ -trastuzumab ( $100 \mu\text{g}, \pm 5 \text{ MBq}$ ) and  $^{111}\text{In}$ -IgG ( $100 \mu\text{g}, \pm 5 \text{ MBq}$ ) co-injection. Post treatment MicroPET scans were acquired according to the same schedule as

described for the baseline scans. NVP-AUY922 treatment was continued till the last scan. After image reconstruction, *in vivo* quantification was performed with AMIDE Medical Image Data Examiner software (version 0.9.1, Stanford University)<sup>17</sup> and tumour accumulation was calculated as standardised uptake value (SUV). Animals were sacrificed after the last scan and organs were excised, rinsed for residual blood, weighed and counted for radioactivity in a calibrated well-type LKB-1282-Compu-gamma system. Tissue activity is expressed as percentage of the injected dose per gram tissue (%ID/g). A separate group of mice receiving only the vehicle was used as control for  $^{89}\text{Zr}$ -trastuzumab and  $^{111}\text{In}$ -IgG biodistribution. Experiments were performed with isofluran inhalation anaesthesia (induction 3%, maintenance 1.5%) and were approved by the animal experiments committee of the University of Groningen.

### 2.7. Immunohistochemistry

Tumours were kept on ice during biodistribution analysis and subsequently processed for immunohistochemical analysis. Formalin-fixed, paraffin-embedded tumours were stained with antibodies against HER2 (HercepTest™, DAKO). Immunohistochemistry results were scored semi quantitatively according to the system used in clinical testing (0, 1, 2 and 3+, which corresponds with no, weak, moderate or strong circumferential, membranous staining).

### 2.8. Statistical analysis

Data are presented as means  $\pm$  standard deviation. Statistical analysis was performed using the Mann-Whitney test for non-parametric data, an unpaired T-test for parametric data and a paired sampled T-test for paired data (SPSS, version 16). A  $p$ -value  $\leq 0.05$  was considered significant.

## 3. Results

### 3.1. NVP-AUY922 downregulates HER2 expression in SKOV-3 cells *in vitro*

NVP-AUY922 induced HER2 downregulation is shown in Fig. 1A. Treatment with 30 and 100 nM NVP-AUY922 for 24 h resulted in HER2 downregulation of  $72.5 \pm 2.4\%$  and  $80.1 \pm 1.4\%$ , respectively, compared with untreated control cells. Treatment with 30, 100 and 500 nM 17-AAG resulted in HER2 downregulation of  $11.4 \pm 3.6\%$ ,  $41.6 \pm 3.7\%$  and  $82.0 \pm 1.2\%$ , respectively, compared with untreated control cells. NVP-AUY922 and 17-AAG isomolar concentrations of 30 and 100 nM resulted in a more pronounced HER2 downregulation after NVP-AUY922 treatment than after 17-AAG treatment with  $p$ -values  $< 0.0001$ . Treatment with 500 nM 17-AAG resulted in similar HER2 downregulation as 100 nM NVP-AUY922 ( $p = 0.15$ ).

### 3.2. NVP-AUY922 reduces $^{89}\text{Zr}$ -trastuzumab binding to SKOV-3 cells *in vitro*

$^{89}\text{Zr}$ -trastuzumab binding to SKOV-3 cells after 24 h treatment with NVP-AUY922, 17-AAG and control is shown in Fig 1B.

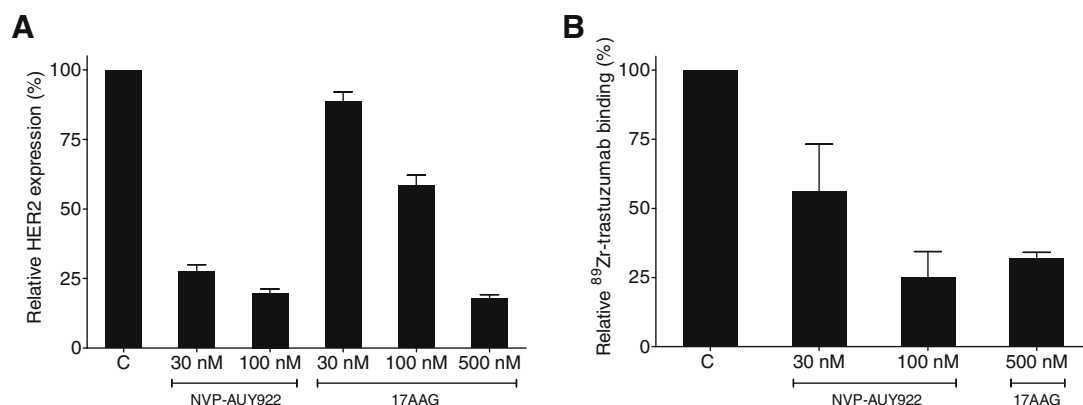


**Fig. 1** – HER2 downregulation, as determined by flow cytometry (A) and <sup>89</sup>Zr-trastuzumab binding, as determined by radio-immuno assay (B), to SKOV-3 after 24 h treatment with NVP-AUY922 and 17-AAG.

Binding of <sup>89</sup>Zr-trastuzumab to untreated SKOV-3 cells was  $21.7 \pm 8.4\%$  of the total <sup>89</sup>Zr-trastuzumab applied. Blocking the cells with an excess of unlabelled trastuzumab reduced <sup>89</sup>Zr-trastuzumab binding to  $0.31 \pm 0.03\%$ , being the non-specific binding of <sup>89</sup>Zr-trastuzumab. Treatment of the cells with 30 and 100 nM NVP-AUY922 reduced the specific binding of <sup>89</sup>Zr-trastuzumab compared to control by  $43.7 \pm 16.9\%$  and  $74.9 \pm 9.3\%$ , respectively. Treatment with 500 nM 17-AAG resulted in a reduction of <sup>89</sup>Zr-trastuzumab specific binding with  $68.2 \pm 2.2\%$ , which was similar to 100 nM NVP-AUY922 ( $p = 0.29$ ).

### 3.3. <sup>89</sup>Zr-trastuzumab PET imaging shows reduced tumour uptake after NVP-AUY922 treatment

Visual analysis of PET imaging showed a time dependent accumulation of <sup>89</sup>Zr-trastuzumab within the tumours. At 144 h post injection, tumour uptake of <sup>89</sup>Zr-trastuzumab was higher than at 72 h post injection. Fig. 2A and B show the transversal and coronal images of a representative mouse scanned at 72 and 144 h post injection of <sup>89</sup>Zr-trastuzumab before and after treatment with NVP-AUY922. Treatment with NVP-AUY922 results in a clearly visible decrease in <sup>89</sup>Zr-trastuzumab tumour uptake. The mean SUV at baseline was

$2.9 \pm 0.6$  and  $3.4 \pm 1.1$  at 72 and 144 h post injection, respectively. The decrease in <sup>89</sup>Zr-trastuzumab tumour uptake after NVP-AUY922 treatment was  $34 \pm 23\%$  ( $p = 0.0009$ ) and  $41 \pm 17\%$  ( $p = 0.0001$ ) at 72 and 144 h post injection, respectively, resulting in a post treatment SUV of  $1.9 \pm 0.8$  and  $2.0 \pm 0.9$  at 72 and 144 h post injection, respectively. Fig. 2C shows the individual tumour SUVs at 144 h post injection of <sup>89</sup>Zr-trastuzumab pre and post treatment with NVP-AUY922.

Biodistribution results in the NVP-AUY922 treatment group ( $n = 10$ ) were compared with the <sup>89</sup>Zr-trastuzumab and <sup>111</sup>In-IgG biodistribution results in a control group ( $n = 7$ ), which received only the vehicle. This comparison was made to determine if the reduced <sup>89</sup>Zr-trastuzumab tumour uptake after NVP-AUY922 treatment was indeed caused by a downregulation of HER2. This proved to be the case as there was a 41% ( $p = 0.0012$ ) lower tumour uptake of <sup>89</sup>Zr-trastuzumab in the NVP-AUY922-treated mice, compared to the control mice (Fig. 3A) whilst there was no difference in <sup>111</sup>In-IgG tumour uptake between treated and control mice. The <sup>89</sup>Zr-trastuzumab tumour uptake was corrected for non-specific uptake by subtracting the <sup>111</sup>In-IgG tumour uptake for each mouse (Fig. 3B). This correction reveals the HER2-driven <sup>89</sup>Zr-trastuzumab tumour uptake which was reduced to 52% ( $p = 0.0002$ ) after NVP-AUY922 treatment, compared to control.

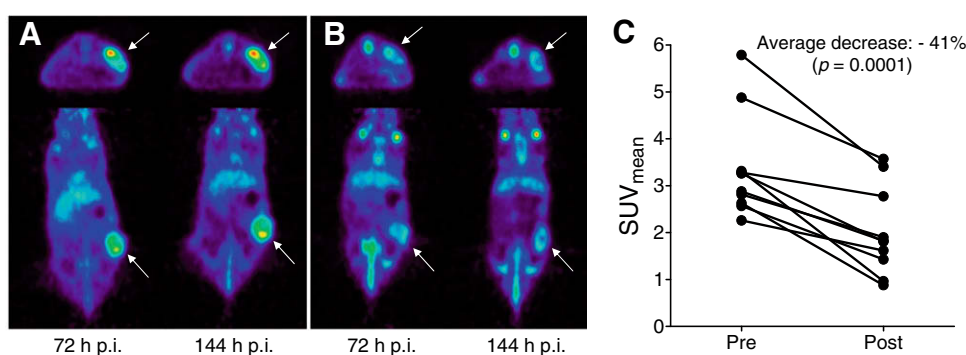


**Fig. 2** – Transversal and coronal PET images of a representative mouse scanned with <sup>89</sup>Zr-trastuzumab before (A) and after (B) treatment with NVP-AUY922. Arrows indicate tumour. PET quantification of <sup>89</sup>Zr-trastuzumab tumour uptake at 144 h post injection is shown in C.

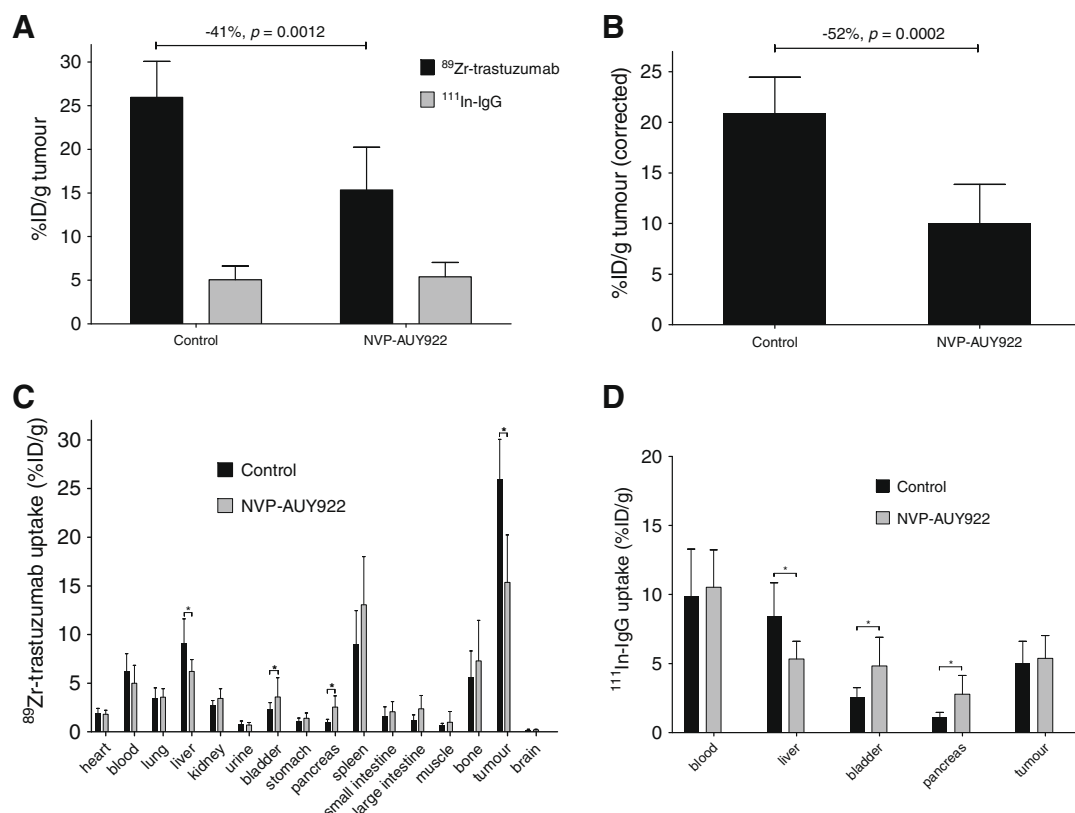


**Fig. 3** –  $^{89}\text{Zr}$ -trastuzumab and  $^{111}\text{In}$ -IgG tumour uptake (A and B) and biodistribution (C and D). Mice were treated with NVP-AUY922 (50 mg/kg, 3qw) or control for 10 d. Both tracers were co-injected at 4 d after initiation of treatment.

The  $^{89}\text{Zr}$ -trastuzumab biodistribution profile at 6 d post tracer injection in treated and control mice shows that NVP-AUY922 affected  $^{89}\text{Zr}$ -trastuzumab uptake in liver, bladder, pancreas and tumour (Fig. 3C).  $^{89}\text{Zr}$ -trastuzumab uptake was higher in bladder and pancreas and lower in liver and tumour in the NVP-AUY922 treated group. These alterations in  $^{89}\text{Zr}$ -trastuzumab uptake in liver, bladder and pancreas were also seen with  $^{111}\text{In}$ -IgG (Fig. 3D), indicating a non HER2-driven mechanism.

### 3.4. Immunohistochemistry

HER2 immunohistochemistry performed on tumours obtained from the biodistribution experiment confirmed the HER2 downregulation in the NVP-AUY922-treated group. All the tumours from the treated mice were still HER2 positive (1+ or 2+), however the HER2 staining in this group was overall less intense compared to the control group (Fig. 4).

## 5. Discussion

In the present study, we successfully demonstrate the feasibility of  $^{89}\text{Zr}$ -trastuzumab HER2 PET as a biomarker for HSP90 inhibition in a HER2 positive xenograft model. Currently there is no clinically proven early biomarker for evaluating the pharmacodynamic effects of HSP90 inhibition. Serial molecular imaging can provide information about the molecular alterations as an early response to HSP90 inhibi-

tion. Because many oncoproteins are clients of HSP90<sup>18,19</sup> there are several molecular imaging target opportunities for non-invasive monitoring of HSP90 inhibition. EGFR imaging with  $^{64}\text{Cu}$ -cetuximab has been used for pharmacodynamic monitoring of 17-AAG in PC-3 human prostate cancer xenografts.<sup>20</sup> However, HER2 imaging is probably a better readout than EGFR imaging since HER2 is likely the client protein most sensitive to HSP90 inhibition and in addition, both nascent and mature HER2 are downregulated by HSP90 inhibition, whereas only nascent EGFR is downregulated.<sup>21</sup> Therefore, for HER2 positive cancers, molecular imaging of HER2 expression during HSP90 inhibiting therapies has the best potential for pharmacodynamic monitoring. This approach has also been evaluated previously in other pre-clinical models. HER2 downregulation induced by 17-AAG in a BT-474 human breast cancer xenograft model was monitored by PET imaging with  $^{68}\text{Ga}$ -DCHF.  $^{68}\text{Ga}$ -DCHF tumour uptake was reduced by 50% after treatment with 17-AAG ( $3 \times 50$  mg/kg in 24 h), compared to baseline  $^{68}\text{Ga}$ -DCHF tumour uptake.<sup>13</sup> In the same xenograft model, the tumour uptake of the metabolic PET tracer [ $^{18}\text{F}$ ]fluorodeoxyglucose (FDG) was unaffected by 17-AAG during the follow-up period of 21 d after treatment.<sup>22</sup> This indicates that HER2 imaging is more useful as an early biomarker for HSP90 inhibition than metabolic FDG imaging.

Radiolabelled full length trastuzumab has been used previously by others to assess HER2 downregulation after HSP90 inhibition. PET imaging with  $^{64}\text{Cu}$ -trastuzumab showed a 64% reduction in tumour uptake 24 h after treatment of



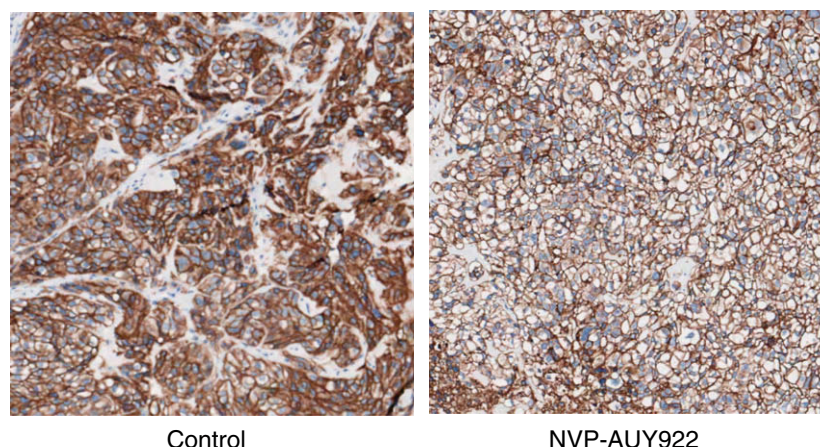


**Fig. 4 – HER2 immunohistochemistry in representative tumours from a control and a NVP-AUY922-treated mouse. Mice were treated with NVP-AUY922 (50 mg/kg, 3qw) or control for 10 d. Tumour samples were collected 2 d after the last dose of NVP-AUY922.**

SKOV-3 xenograft bearing mice with 17-(dimethylaminoethyl)-17-demethoxygeldanamycin (17-DMAG; alvespimycin) ( $3 \times 50$  mg/kg in 24 h).<sup>23</sup> Similar results were seen with HER2 PET imaging using the  $^{18}\text{F}$ -FBEM- $\text{Z}_{\text{HER2:342}}$  affibody molecule after treatment of BT-474 xenografts with 17-DMAG (40 mg/kg/d, 4 doses).<sup>24</sup>

NVP-AUY922 induced downregulation of HER2 was first shown in HCT116 colon carcinoma cells by Western blot analysis.<sup>6</sup> In a BT-474 human breast cancer xenograft model, a single dose of 50 mg/kg NVP-AUY922 resulted in a HER2 downregulation, as determined with immunohistochemistry and Western blot.<sup>8</sup> Our *in vitro* results confirm the HER2 downregulation by NVP-AUY922, which was more potent than that of 17-AAG in isomolar concentrations. It should be noted that NVP-AUY922 is a very promising HSP90 inhibitor, which shows considerably less toxic effects than the geldanamycin derivatives in the current clinical phase I evaluation.

Our *in vivo* results show an average decrease of 41% in  $^{89}\text{Zr}$ -trastuzumab tumour uptake, which is comparable with the decrease which was reported with  $^{68}\text{Ga}$ -DCHF,  $^{18}\text{F}$ -FBEM- $\text{Z}_{\text{HER2:342}}$  and  $^{64}\text{Cu}$ -trastuzumab after HSP90 inhibiting treatment. Main difference between  $^{68}\text{Ga}$ -DCHF,  $^{18}\text{F}$ -FBEM- $\text{Z}_{\text{HER2:342}}$ ,  $^{64}\text{Cu}$ -trastuzumab and  $^{89}\text{Zr}$ -trastuzumab HER2 PET imaging is the interval between tracer injection and scan acquisition, which is limited by the physical half-life of the radioisotopes. Half-lives of 1.13 and 1.83 h limit imaging with  $^{68}\text{Ga}$ -DCHF and  $^{18}\text{F}$ -FBEM- $\text{Z}_{\text{HER2:342}}$  to several hours post tracer injection, where the half-life of  $^{64}\text{Cu}$  of 12.7 h allows trastuzumab imaging up to 48 h. We performed HER2 PET imaging in metastatic breast cancer patients up to 7 d post injection of  $^{89}\text{Zr}$ -trastuzumab (with a half-life of 78.4 h) and found that the best images were obtained on days 4 and 5.<sup>15</sup> This is in accordance with the fact that antibodies like trastuzumab accumulate slowly into the tumours, which makes trastuzumab imaging days after injection more rational. Our imaging data with  $^{89}\text{Zr}$ -trastuzumab in the present study were acquired 72 and 144 h post tracer injection during treatment with NVP-AUY922 every 48 h. These data showed still an increase over time of  $^{89}\text{Zr}$ -trastuzumab tumour uptake from 72 to 144 h. The effect of NVP-AUY922 on  $^{89}\text{Zr}$ -trastuzumab

tumour uptake was most pronounced at 144 h post tracer injection. The tumour uptake of  $^{89}\text{Zr}$ -trastuzumab at 144 h p.i. reflects the level of HER2 membrane expression during that 144 h, which will be the integrated result of NVP-AUY922 induced HER2 downregulation over this interval.

Even though HER2 may serve as an excellent read out for HSP90 inhibition, it is not universally expressed in tumour tissue. Therefore, also other client proteins are of interest in this setting. In our institution, we have also studied the effect of HSP90 inhibition on VEGF expression by means of  $^{89}\text{Zr}$ -bevacizumab PET in a pre-clinical model. An advantage of this marker is that it is universally expressed in tumours, although VEGF may not be as sensitive as readout compared to HER2. HER2 imaging is readily available for use in patients in our institution, and at present we are translating these pre-clinical results to the clinical setting in collaboration with the Royal Marsden institute in London.

In summary, this paper describes the successful pre-clinical validation of  $^{89}\text{Zr}$ -trastuzumab HER2 PET for non-invasive pharmacodynamic monitoring of the HER2 downregulation by the HSP90 inhibitor NVP-AUY922. This technique might serve as an early biomarker for HSP90 inhibition in HER2 positive metastatic breast cancer patients and could potentially support patient tailored therapy.

### Conflict of interest statement

M.R.J. and C.Q. are employees of Novartis.

### Role of the funding source

Personnel (TOM) and materials were paid from the Dutch Cancer Society grant. Novartis provided NVP-AUY922.

### Acknowledgements

The authors would like to thank Kirsten van Huisstede and Esther van Straten for their technical assistance. This work was supported by grant 2007-3739 of the Dutch Cancer Society.

## REFERENCES

1. Workman P, Burrows F, Neckers L, Rosen N. Drugging the cancer chaperone HSP90: combinatorial therapeutic exploitation of oncogene addiction and tumor stress. *Ann NY Acad Sci* 2007;**1113**:202–16.
2. Ferrarini M, Heltai S, Zocchi MR, Rugarli C. Unusual expression and localization of heat-shock proteins in human tumor cells. *Int J Cancer* 1992;**51**:613–9.
3. Kamal A, Thao L, Sensintaffar J, et al. A high-affinity conformation of Hsp90 confers tumour selectivity on Hsp90 inhibitors. *Nature* 2003;**425**:407–10.
4. Banerji U, O'Donnell A, Scurr M, et al. Phase I pharmacokinetic and pharmacodynamic study of 17-allylamino, 17-demethoxygeldanamycin in patients with advanced malignancies. *J Clin Oncol* 2005;**23**:4152–61.
5. Modi S, Stopeck AT, Gordon MS, et al. Combination of trastuzumab and tanespimycin (17-AAG, KOS-953) is safe and active in trastuzumab-refractory HER-2 overexpressing breast cancer: a phase I dose-escalation study. *J Clin Oncol* 2007;**25**:5410–7.
6. Brough PA, Aherne W, Barril X, et al. 4, 5-diarylisoazole Hsp90 chaperone inhibitors: potential therapeutic agents for the treatment of cancer. *J Med Chem* 2008;**51**:196–218.
7. Eccles SA, Massey A, Raynaud FI, et al. NVP-AUY922: a novel heat shock protein 90 inhibitor active against xenograft tumor growth, angiogenesis, and metastasis. *Cancer Res* 2008;**68**:2850–60.
8. Jensen MR, Schoepfer J, Radimerski T, et al. NVP-AUY922: a small molecule HSP90 inhibitor with potent antitumor activity in preclinical breast cancer models. *Breast Cancer Res* 2008;**10**:R33.
9. Seddon BM, Workman P. The role of functional and molecular imaging in cancer drug discovery and development. *Br J Radiol* 2003;**76**(Spec. no. 2):S128–38.
10. Moasser MM. The oncogene HER2: its signaling and transforming functions and its role in human cancer pathogenesis. *Oncogene* 2007;**26**:6469–87.
11. Solit DB, Zheng FF, Drobnjak M, et al. 17-Allylamino-17-demethoxygeldanamycin induces the degradation of androgen receptor and HER-2/neu and inhibits the growth of prostate cancer xenografts. *Clin Cancer Res* 2002;**8**:986–93.
12. Zsebk B, Citri A, Isola J, Yarden Y, Szollosi J, Vereb G. Hsp90 inhibitor 17-AAG reduces ErbB2 levels and inhibits proliferation of the trastuzumab resistant breast tumor cell line JIMT-1. *Immunol Lett* 2006;**104**:146–55.
13. Smith-Jones PM, Solit DB, Akhurst T, Afroze F, Rosen N, Larson SM. Imaging the pharmacodynamics of HER2 degradation in response to Hsp90 inhibitors. *Nat Biotechnol* 2004;**22**:701–6.
14. Dijkers ECF, Kosterink JG, Rademaker AP, et al. Development and characterization of clinical-grade <sup>89</sup>Zr-trastuzumab for HER2/neu immunoPET imaging. *J Nucl Med* 2009;**50**:962–9.
15. Oude Munnink TH, Dijkers ECF, Lub-De Hooge MN, et al. HER2 PET imaging with <sup>89</sup>Zr-trastuzumab in metastatic breast cancer patients. *J Clin Oncol* 2009;**27**(15S) [abstract #1045].
16. Ruegg CL, Anderson-Berg WT, Brechbiel MW, Mirzadeh S, Gansow OA, Strand M. Improved in vivo stability and tumor targeting of bismuth-labeled antibody. *Cancer Res* 1990;**50**:4221–6.
17. Loening AM, Gambhir SS. AMIDE: a free software tool for multimodality medical image analysis. *Mol Imaging* 2003;**2**:131–7.
18. Goetz MP, Toft DO, Ames MM, Erlichman C. The Hsp90 chaperone complex as a novel target for cancer therapy. *Ann Oncol* 2003;**4**:1169–76.
19. Calderwood SK, Khaleque MA, Sawyer DB, Ciocca DR. Heat shock proteins in cancer: chaperones of tumorigenesis. *Trends Biochem Sci* 2006;**31**:164–72.
20. Niu G, Cai W, Chen K, Chen X. Non-invasive PET imaging of EGFR degradation induced by a heat shock protein 90 inhibitor. *Mol Imaging Biol* 2008;**10**:99–106.
21. Xu W, Mimnaugh E, Rosser MF, et al. Sensitivity of mature ErbB2 to geldanamycin is conferred by its kinase domain and is mediated by the chaperone protein Hsp90. *J Biol Chem* 2001;**276**:3702–8.
22. Smith-Jones PM, Solit D, Afroze F, Rosen N, Larson SM. Early tumor response to Hsp90 therapy using HER2 PET: comparison with <sup>18</sup>F-FDG PET. *J Nucl Med* 2006;**47**:793–6.
23. Niu G, Li Z, Cao Q, Chen X. Monitoring therapeutic response of human ovarian cancer to 17-DMAG by noninvasive PET imaging with <sup>64</sup>Cu-DOTA-trastuzumab. *Eur J Nucl Med Mol Imaging* 2009; published online, May 14.
24. Kramer-Marek G, Kiesewetter DO, Capala J. Changes in HER2 expression in breast cancer xenografts after therapy can be quantified using PET and <sup>18</sup>F-labeled affibody molecules. *J Nucl Med* 2009;**50**:1131–9.